

1 " Characterization of evolutionarily conserved *Trypanosoma cruzi* NatC and NatA-
2 N-terminal acetyltransferase complexes."

3 Stephen Ochaya^{1,7*}, Oscar Franzén¹, Doreen Asiimwe Buhwa⁵, Håvard Foyn³, Claire
4 E. Butler⁶, Svein Isungset Stove^{3,8}, Kevin M. Tyler ⁶, Thomas Arnesen^{3,4,8}, Enock
5 Matovu⁵, Lena Åslund² and Björn Andersson^{1*}.

6 1- Department of Cell and Molecular Biology, Karolinska Institutet, Box 285, SE-171
7 77 Stockholm, Sweden.

8 2- Department of Immunology, Genetics and Pathology, Rudbeck Laboratory, S-
9 75185 Uppsala, Sweden.

10 3- Department of Biological Sciences, University of Bergen, N-5020 Bergen, Norway.

11 4- Department of Surgery, Haukeland University Hospital, N-5020 Bergen, Norway.

12 5- Department of Parasitology and Microbiology, Makerere University, P.O. Box
13 7062, Kampala, Uganda.

14 6- Biomedical Research Centre, Norwich Medical School, University of
15 East Anglia, Norwich, Norfolk, NR4 7TJ, UK.

16 7- Department of Immunology and Microbiology, Gulu University, P.O. Box 166
17 Gulu, Uganda.

18 8- Department of Biomedicine, University of Bergen, N-5020 Bergen, Norway.

19 Authors e-mail

20 SO: sstephen.ochaya@gmail.com

21 OF: p.oscar.franzen@gmail.com

22 HF: havard.foyn@ncmm.uio.no

23 SS: svein.stove@mbi.uib.no

24 DB: buhwa@yahoo.com

25 CB: claire.angell.uk@gmail.com

26 KT: K.Tyler@uea.ac.uk

27 EM: matovue@covab.mak.ac.ug

28 TA: thomas.arnesen@mbi.uib.no

29 LA: lena.aslund@igp.uu.se

30 BA: bjorn.andersson@ki.se

31 * Corresponding authors: Stephen Ochaya and Björn Andersson

32 **Key words:** *Trypanosomes*, Acetyltransferase, N^{α} -acetyltransferase gene/protein, N^{α}
33 -terminal acetylation, RNAi

35 **Abstract**

36 Protein N-terminal acetylation is a co- and post-translational modification, conserved
37 among eukaryotes. It determines the functional fate of many proteins including their
38 stability, complex formation and subcellular localization. N-terminal
39 acetyltransferases (NATs) transfer an acetyl group to the N-termini of proteins, and
40 the major NATs in yeast and humans are NatA, NatB and NatC. In this study, we
41 characterized the *Trypanosoma cruzi* (*T. cruzi*) NatC and NatA protein complexes,
42 each consisting of one catalytic subunit and predicted auxiliary subunits. The proteins
43 were found to be expressed in the three main life cycle stages of the parasite, formed
44 stable complexes *in vivo*, and partially co-sedimented with the ribosome in agreement
45 with a co-translational function. An *in vitro* acetylation assay clearly demonstrated
46 that the acetylated substrates of the NatC catalytic subunit from *T. cruzi* were similar
47 to those of yeast and human NatC, suggesting evolutionary conservation of function.
48 An RNAi knockdown of the *Trypanosome brucei* (*T. brucei*) NatC catalytic subunit
49 indicated that reduced NatC-mediated N-terminal acetylation of target proteins reduce
50 parasite growth.

1. Introduction

Trypanosomes are protozoan parasites that can cause severe health problems, mainly in developing countries. *Trypanosoma cruzi* is the causative agent of Chagas disease, common throughout Latin America; while *T. brucei*, mainly present in Africa, causes sleeping sickness in humans and Nagana in livestock (1) (2). There is no vaccine against trypanosome-related diseases and the available drugs cause serious side effects (3)(4). The study about N-terminal acetylation as a possible chemotherapeutic target to fight parasite infections is limited. Protein N α -acetylation (Nt-acetylation) is an irreversible protein modification where the acetyl moiety is transferred to the N α amino group of a protein or polypeptide by N-terminal acetyltransferases (NATs). NATs are grouped according to their substrate specificity. In humans, seven NATs have been identified so far (NatA-F, and NatH) (5)(6). Of these, NatA, NatB and NatC have the largest number of substrates and have been characterized extensively. The human NatA protein complex is composed of a catalytic subunit (hNaa10) and an auxiliary subunit (hNaa15) and the human NatC consists of a catalytic (hNaa30) subunit and two auxiliary (hNaa35 and hNaa38) subunits (7)(8). The proteins form stable complexes *in vivo* and co-sediment with the ribosome (9)(8). Of late, studies exploring the biological significance of NATs have become topical, in particular with regard to how they contribute to cellular integrity and their roles in cancer (10)(11). At the substrate protein level, Nt-acetylation may act as a degradation signal (12), mediate protein complex formation (13) or inhibit post- translational ER-translocation (14). Indeed, both human NatC and NatA have been suggested as possible target to control cancer (8)(15).

N-terminal acetyltransferases (NATs); the co- and post-translational modification is common in all kingdoms of life. About 60 %, 90 %, 75 %, and 18 % of yeast, human, plant and archea proteins, respectively, are thought to be Nt-acetylated (16)(17)(5).

The NatA complex from *T. brucei* has been found to be essential for cell viability in both the mammalian and insect stages (18). We previously characterized a novel acetyltransferase, the catalytic subunit of the NatC complex in *T. cruzi* (19), thought to belong to the NatC subgroup. In the present study, we have characterized and begun to investigate the biological significance of the predicted NatC and NatA in *T. cruzi*.

We demonstrate that the catalytic subunits (TcNaa10) and (TcNaa30), and the predicted auxiliary subunits are expressed and co-sediment with the ribosome. We find that TcNaa30 catalyzes the acetylation of N-termini similar to those acetylated by NatC in yeast (yNaa30) and hNaa30 *in vitro* and our analyses indicate that the protein may function both as a N α - and as a N ϵ - acetyltransferase. Finally, there is an indication that the knockdown of the *T. brucei* NatC catalytic subunit is important to the parasite.

2. Materials and Methods.

2.1 Cell culture.

T. cruzi CL Brener epimastigotes were cultured as previously described (19). Tissue culture derived trypomastigotes were obtained through infection of a Vero cell monolayer, harvesting the media by centrifugation at 1640 g for 10 min. Amastigotes were obtained by harvesting 5 x 10⁶ trypomastigotes per ml and incubating in serum-free DMEM for 48 h at 37 °C. Metacyclogenesis was induced by separating 5 x 10⁶ epimastigotes per ml into Grace's insect medium supplemented by intestinal homogenate from *Rhodnius prolixus* (20) and 0.5 % pyruvate-glutamate-antibiotic (PGAB). *T. brucei* strains were grown in HM-I9 medium at 37 °C, 5 % CO₂.

2.2 Identification, cloning and expression of suspected TcNatC and TcNatA subunits.

Human Mak3 (hNaa30), gene ID 122830 and hNaa38 (NP_001317040.1 GI:1052793474) sequences were BLASTed against the *T. cruzi* CL Brener proteome in order to identify *T. cruzi* homologs of NatC catalytic and an auxiliary subunit. Similarly, the second TcNatC auxiliary subunit was identified using plant Mak10 acetyltransferase (*Arabidopsis thaliana*) NP_001118295.1, GI:186500070 or *Rattus norvegicus* NP_579858.1 GI:19033372. The auxiliary subunits were amplified from total genomic DNA from Sylvio strain (TcI) using the following primers TcNATC mak10 Forward: 5' CGAATTCATGGCGTGTGACCTTGA 3', and TcNATC mak10 Reverse: 5' GAGCGGCCGCTTACCTGGCTTCCTTCTTG 3', with EcoR1 and NotI restriction sites (underlined), respectively. And, TcLsmd1 Forward: 5' GGAATTCATGGGCCGCGAGAGCATGCTTCACAA 3' and TcLsmd1 Reverse: 5' AAGCTCGAGTTAGCGCTTCCGCTT 3', with EcoR1 and XhoI restriction sites (underlined). The genes were cloned into pGEX5-1 vector expressing GST (glutathione S-transferase) and recombinant proteins were produced. The pelleted

bacteria was dissolved in PBS containing EDTA-free protease inhibitor tablets (Roche), 1 mM EDTA, 100 µg lysozyme and incubated on ice for about 15 min. Sarkosyl was added to a concentration of 1.5 %. The cells were briefly sonicated four times, 10 s each, with 30 s pauses using Branson sonifier cell disruptor B 15. The pellet and supernatant were analyzed to detect the presence of the induced protein.

For the TcNatA subunits, human or yeast NatA sequences were used as queries in the NCBI BLAST database in order to identify TcNatA homologues. *T. cruzi* gene TcCLB.506227.230 (predicted catalytic subunit, which we named TcNaa10) and gene TcCLB.510301.80 (predicted auxiliary subunit, named TcNaa15) were identified. The genes were amplified from genomic DNA using the following primers: TcNAA10 Forward: 5' **AAGAATTC**ATGCAGATCCGTCGC 3', TcNAA10 Reverse: 5'AA**ACTCGAGT**CACTTTTTCGTCTTGCC 3', TcNAA15 Forward: 5'ATCG**GAATTC**CGGTAGTGCTTCCTCCGGCG 3', and TcNAA15 Reverse: 5'ATCG**CTCGAG**GCGCTGGCCAACACCTCATCA 3'. Bold and underlined are EcoRI (forward) and XhoI (reverse) restriction sites.

The genes were subsequently cloned into the pGEX5-1 vector expressing GST (glutathione S-transferase) yielding pGEX5-1-TcNaa10 and pGEX5-1-TcNaa15. The reading frames were confirmed as described previously (19). Bacterial Top10 cells (Invitrogen) transformed with pGEX5-1-TcNaa10, were grown at 37 °C until approximately OD₆₀₀ 0.5 and induced with 0.3 mM isopropyl β-D-1-thiogalactopyranoside (IPTG). Cells were grown and processed as described before (19), except that protease inhibitor (EDTA-free tablet inhibitor from Roche) was used. The bacterial Top10 cells (Invitrogen) transformed with pGEX5-1-TcNaa15, were grown to approximately OD₆₀₀ 0.8 and induced with 0.1 mM IPTG at 24 °C for about 24 h, and further processed as was done for pGEX5-1-TcNaa10.

2.3 Generation of anti-TcNaa10, TcNaa15 and anti-TcNaa38 antibodies and western blot analysis.

The antibody production for TcNaa10 and TcNaa38 was performed in a rabbit by Innovagen (Lund, Sweden), as before (19). Protein G was used to purify the IgGs. The anti-GST antibodies were removed by passing the immunoglobulin through a GST-column. The depletion and titer were evaluated by immunoblotting to GST and GST-TcNaa38, GST-TcNaa10 electrotransferred strips (not shown). Antibody against

TcNaa15 was generated by the Agrisera company (Umeå-Sweden) by inoculating one rabbit with synthetic peptides: Naa15-EL (700-712) (NH₂-) CDEVLASAWEKIKE (-COO). The peptide sequence was selected from conserved regions from both CL Brener haplotypes (non- Esmeraldo and Esmeraldo like). Western blotting was performed using standard procedures and as before (19). The anti-TcNaa10, anti-TcNaa15 and anti-TcNaa38 antibodies were used at a dilution of 1:4000, 1:2000 and 1:2000, respectively. For comparison between life cycle stages, fractions containing 10⁶ cells was lysed directly in sample loading buffer and separated on a 15 % acrylamide gel. Proteins were transferred using a semi-dry system and the membrane probed with for example, anti-TcNaa38 overnight.

2.4 *In vitro* acetylation assay.

E. coli cells harboring the expression plasmid pGEX5-TcNaa30 were grown at 37 °C in Luria-Bertani medium containing appropriate amounts of ampicillin. Expression was induced at approximately 0.5 OD₆₀₀ by the addition of 0.3 mM IPTG and growth was continued for additional 18 h at 17 °C, 190 rpm. The cells were processed as described previously (19).

The enzyme activity of purified GST-TcNaa30 was determined as described in (8). In brief, GST-TcNaa30 was mixed with potential oligopeptide substrates (300 mM) and acetyl-CoA (300 mM) in a total volume of 60 µl acetylation buffers. The samples were incubated at 37 °C for 30 min. The enzyme activity was quenched by adding 5 µl of 10 % TFA. The amount of acetylated oligopeptides was determined based on the absorbance at 215 nm after analysis with RP-HPLC. Synthetic Peptide Sequences used were as described elsewhere (8) (7).

To assess the TcNaa10 acetyltransferase activity, recombinant protein was expressed as described above, except that growth was continued for another 25 h at 17 °C, 189 rpm. The cells were chilled on ice and harvested by centrifugation at 5000 rpm for 15 min. The cell pellet was suspended in 5 ml of ice-cold PBS containing EDTA-free tablets inhibitor (Roche). Cells were sonicated 4 times, 10 s each using a Branson sonifer cell disruptor B 15. Five ml of cold PBS + inhibitor, 0.5 ml of 20 % Triton X-100 (final conc. 1 %) was added and the cells were incubated for 30 min at 4 °C and thereafter centrifuged for 15 min at 10,000 rpm. From a 50 % slurry of glutathione-Sepharose 4B (GE Healthcare), about 250 µl were added to the supernatant and the

mixture was incubated for 2-3 h at 4 °C. The beads were washed three times with cold PBS containing 1 % Triton X-100, followed by one wash with PBS. The amount of protein on the beads was estimated from Coomassie staining of SDS-PAGE gels.

The purified recombinant protein (GST-TcNaa10), eluted from the beads, was incubated with Acetyl-CoA and synthetic peptides suggested to be the substrates for NatA. The activity of the enzyme was stopped after 30 min and the results analyzed by HPLC.

2.5 Immunofluorescence microscopy.

Parasites were prepared for IF essentially as previously described (21), fixing in 4 % paraformaldehyde for 5 min. Cells were then blocked in 10 % goat serum and primary antibodies were used at a 1:50 dilution for 1 h. Anti-rabbit AlexaFluor488 was used to recognize the primary antibodies and cells were DAPI stained prior to mounting in Fluoromount. Imaging was achieved using a Zeiss Axioplan2 microscope and Axiovision 4.7 software.

2.6 Immunoprecipitation (IP).

Approximately 10^9 parasites per ml were used for immunoprecipitation. Exponentially growing cells were lysed in lysis buffer [0.75 % CHAPS detergent, 1 mM MgCl₂, 1 mM EGTA, 5 mM β -mercapthoethanol, 10 mM Tris-HCL (pH 7.6), 10 % glycerol and 1 mM Pefabloc (Roche)]. The sample was incubated on ice and later centrifuged. The supernatant was pre-cleared by incubation with protein A/G–agarose (Santa Cruz Biotechnology) on a roller for 1 h at 4 °C. The beads were removed by centrifugation at 1000 g for 3 min. The cell lysate was incubated with about 2 μ g of anti-TcNaa10, or anti-TcNaa30 antibody. As a control, one part of the lysate was incubated with rabbit sera (pre- immune). Both samples were incubated on a roller for about 2.5 h at 4 °C before adding 30 μ l of Protein A/G– agarose beads and further incubated overnight at the same temperature. The beads were collected by centrifugation as above, washed, mixed with sample buffer and boiled for 10 min. After centrifugation, the supernatant was analyzed by SDS/PAGE and western blotting. Reciprocal IP with anti-TcNaa15, or anti-TcNaa38 was done as described except that in this case, the lysate was not pre-cleared.

2.7 Polysome Isolation.

Total ribosome isolation was performed using a modification of previously described methods (8). Approximately 10^9 cells were used per experiment. Prior to harvesting, parasites were treated with 100 μ g/ml cycloheximide (CHX) for about 10 min on ice. Cells were then lysed with KCl ribosome lysis buffer (8) and incubated on ice for 15 min. Cells were homogenized by repeated pipetting and the homogenate verified with light microscopy. The lysate was centrifuged at 18000 g at 4 °C for 5 min using Beckman rotor 25.50. One ml of the lysate was overlaid on 3 ml of 25 % sucrose cushion sucrose and ultra-centrifuged at 135,715.5 g for 2 h using Sorvall AH-650 rotor (Beckman) .The pellet was dissolved in ribosomal lysis buffer. Total parasite lysate, top supernatant (post-polysome lysate) and ribosomal pellet were analyzed by SDS-PAGE and western blotting.

2.8 Nuclear and cytoplasmic preparation.

About 10^7 exponentially growing parasites were washed twice in PBS and lysed in 10 μ l of TELT buffer (50 M Tris-HCL pH 8, 62.5 mM EDTA, 2.5 M LiCl, 0.4 % Triton X-100 and 100 mg/ml lysozyme). Thereafter, NE-PER Nuclear and Cytoplasmic Extraction Reagents kit from Thermo Scientific was used according to recommendation, but with double amount of reagents. Prior to the use of the kit, the parasites were lysed by TELT, as the detergent provided with the kit did not lyse the parasite at the condition tested. Anti-cyclophilin A (kindly provided by Jacqueline Búa, Instituto Nacional de Parasitologia, Buenos Aires, Argentina) and anti- histone 3 from Upstate (Millipore) were used as positive control for cytoplasmic and nuclear proteins, respectively.

2.9 Bioinformatics.

Homology searches were performed using the NCBI BLAST server. Extracted protein sequences were aligned using Clustal Omega multiple sequence alignment tool. ScanProsite and InterPro Protein sequence analysis and classification tools were used to identify domains.

2.10 Generation of predicted T. brucei NatC catalytic subunit (TbNaa30) RNAi cell lines.

The putative protein-coding region comprising nucleotides (216-788) of the predicted TbNaa30 (Tb927.7.2360), that is, a 573 bp fragment, was PCR-amplified using forward primer TbNatC-Naa30RNAi:

5'ATCGGGATCCCTACGGATGTCGCTCCTAGC 3' and reverse primer TbNatC-Naa30RNAi: 5' ATCGAAAGCTTGTAGCGCGGCAGAAATTTAG 3'. Underlined are BamHI and Hind III restriction sites, respectively. The PCR product was subcloned into tetracycline- inducible RNAi vector p2T7-177 using the restriction sites to yield p2T7-TbNaa30. The presence of the insert was verified by digesting the plasmid with respective enzymes. For easy incorporation into the chromosome, resulting plasmid (about 10 µg) was linearized with NotI and transfected into *T. brucei brucei* 427 strain by electroporation, using about 2×10^7 cells. Non-linearized plasmid and mock transfection were used as negative controls. The transformants were selected with phleomycin (2.5 µg). To confirm if the transfection was successful, DNA was extracted from the surviving parasites and PCR was performed to amplify the phleomycin gene fragment (350 bp) using specific primers (Phleo Forward 5' ATG GCC AAG TTG ACC AGT GCC 3' and Phleo Reverse 5' TGC ACG CAG TTG CCG GCC GGG 3'). The starting parasite density of 2.5×10^4 /ml was used and RNAi was induced using 100 ng of tetracycline. The same parasite density was used for the transformants and wild type (*T. b. brucei* 427). The non-induced/wild type and induced cells were examined and counted daily using light microscopy. Samples for gene/protein expression analyses were harvested daily for five days.

3. Results

3.1 Identification and sequence analysis of TcNat proteins.

The catalytic subunit of the TcNatC complex was identified by blast analysis and as previously described (19) (table 1). In accordance with the recommended nomenclature (22), we now refer to this gene as TcNaa30. Similarly, we identified putative genes for the *T. cruzi* homologues of NatC auxiliary subunits (TcNaa35 and TcNaa38), (table 1). The gene showed 19 %, 22 %, 49 % and 62 % sequence identity at the aa level to its rat, plant, *Leishmania major* and *T. brucei* counterpart, respectively. For TcNaa38, gene Tc00.1047053507209.10 (Tc9.10) was identified as the likely TcNatC subunit, (table 1). At the aa level, the TcNaa38 gene shares, 32 %, 38 %, 57 % and 62 % sequence identity with its yeast, human, *Leishmania major* and *T. brucei* counterpart, respectively.

T. cruzi NatA homologs were identified by comparing with human Naa10, (gene ID 728880) (table 1). The *T. cruzi* gene TcCLB.506227.230 (Tc7.230) was found to

share 60 % and 42 % identity at the amino acid (aa) level with the human and yeast genes, respectively. We now refer to this gene as TcNaa10 according to the latest nomenclature (22). In a search to identify the *T. cruzi* NatA auxiliary subunit, we used hNaa15 (NP_476516.1), as a BLAST query sequence. As seen in (table 1), the search identified CL Brener gene TcCLB.504163.110 (Tc3.110) and TcCLB.510301.80 (Tc01.80), with 29 % and 28 % sequence identity at the aa level, respectively. Both alleles were annotated as putative N-acetyltransferase subunit Nat1 and named TcNaa15. Sequence comparison of predicted TcNaa35, TcNaa38, TcNaa10 and TcNaa15 with selected species is displayed in (Supplementary Fig. S1).

3.2 Expression and recombinant production of TcNatA and TcNatC protein subunits.

We previously expressed the putative TcNaa30 and showed that it has auto-acetylation enzyme activity (19). To further characterize the TcNatC and TcNatA protein complex, we cloned the TcNaa35 and TcNaa38 ORFs and produced recombinant protein. (Supplementary Fig. S2A and S2B) show the recombinant protein (GST- TcNaa35 and GST-TcNaa38) with an expected size of about 110 and 40 kDa, respectively. The annotated proteins of TcNaa10 and TcNaa15 have predicted molecular weights of 29.4 and 82.9 kDa, respectively, and we again produced recombinant proteins. TcNaa10 was initially insoluble (Supplementary Fig. S2C and S2D) and was dissolved in sarkosyl as described previously (25).

3.3 Expression of TcNaa38/TcNaa30 and TcNaa10/TcNaa15 in the parasite.

To investigate the expression pattern of TcNatC and TcNatA, we used western blot to detect the proteins in the different stages of the parasite life cycle. In the study, polyclonal antibodies were produced in rabbit against the whole protein. **The antibody against TcNaa15 was generated in a rabbit using synthetic peptides.** ~~But, inoculating one rabbit with synthetic peptides generated antibody against TcNaa15.~~ For all the proteins assessed, we first carried out western blot analysis for pre-immune rabbit sera, and as expected, no band /signal was detected (not shown).

Analysis showed that TcNaa38 was expressed in the three main stages, *i.e.* in the epimastigote, trypomastigote and amastigote stages of *T. cruzi* CL Brener (Figure 1(A)). However, multiple bands of similar size were recognized in all the stages, possibly due to **post- translational processing of proteins.** ~~the hybrid nature of CL Brener strain.~~ The identity of the extra bands has not been investigated in this study.

Anti-TcNaa38 and anti-TcNaa30 also recognized, for example GVR35 (26) and URTO (27) strains of *T. brucei* proteins (Figure 1(B)). TcNaa10/TcNaa15 were also found to be expressed in epimastigote, trypomastigote and amastigote stages of the *T. cruzi* CL Brener strain (Figure 1(C)). ~~But, except for amastigote, extra bands could be seen for a~~ Anti-TcNaa15 detected additional bands in all developmental stages, except amastigotes. The identities of these bands are not known. Furthermore, the result suggests an up-regulation of TcNaa15 in the trypomastigote and amastigote stages with an opposite effect seen for TcNaa10, that is, down-regulated in trypomastigotes and amastigotes (Figure 1(C)). As displayed in (Figure 1(D)), anti-TcNaa10 was found to cross react with *T. brucei*, while anti-TcNaa15, as expected, did not. ~~because specific peptide sequence was selected from CL Brener haplotypes to generate the antibody used in the experiment.~~ In contrast to *T. cruzi*, anti-TcNaa10 recognized an extra band of 17 kDa in *T. brucei*, with no known identity. Taken together, the results indicate that the TcNatA and TcNatC protein complexes are constitutively expressed in *T. cruzi*.

3.4 Localization of TcNaa30 and TcNaa10/TcNaa15 by fractionation.

~~The staining profile of the putative TcNaa30 was previously shown to be predominantly located in the cytoplasm~~ As shown in (19), the staining profile of the putative TcNaa30 was predominantly located in the cytoplasm, and we now observed the same result by fractionation (Figure 2(A)). For TcNaa15 and TcNaa10, both proteins showed nuclear and cytoplasmic location (Figure 2(B)).

3.5 Subcellular localization of TcNaa30 /TcNaa38 and TcNaa10/TcNaa15 by immunofluorescence.

In assessing all the staining patterns assessed for of the four proteins, ~~not that~~, no staining was observed by pre-immune sera, or by secondary antibody alone (data not shown). In both midlog and stationary epimastigotes, the TcNaa30 exhibited some perinuclear accumulation and punctate structures ~~could be observed~~, particularly in the stationary phase (Figure 3(A)). In both metacyclic and tissue culture derived trypomastigotes, TcNaa30 appeared to be relatively sequestered in a perinuclear distribution, as was observed in (28). When trypomastigotes were differentiated into amastigotes *in vitro*, however, more peripheral staining was observed (Figure 3(A)).

These differences could possibly be related to differential regulation of protein trafficking.

TcNaa38 staining was predominantly punctate and cytoplasmic labeling more diffuse at the midlog stages (Supplementary Fig. S3A). Tissue culture derived trypomastigotes showed a diffuse cytoplasmic localization with some perinuclear accumulation. In amastigotes *in vitro*, TcNaa38 staining was again punctate and cytoplasmic (Supplementary Fig. S3A). Using a Vero cell monolayer to assess intracellular amastigotes, the staining profile showed a diffuse localization of TcNaa30 in the cytoplasm, and a more punctuated labeling for TcNaa38 (Supplementary Fig. S4).

The localization pattern of TcNaa10 and TcNaa15 *in vivo* in the four developmental stages of the parasite were assessed. TcNaa10 was mainly seen around the nucleus in midlog and stationary epimastigotes (Figure 3(B)). In trypomastigotes, TcNaa10 appeared exclusively around the nucleus (Figure 3(B)). The staining profile of TcNaa10 in amastigotes meanwhile, was restricted to the periphery of the cell (Figure 3(B)). In all the life cycle stages, TcNaa15 appeared to predominantly localize to the cell periphery (Supplementary Fig. S3B). The cytoplasmic labeling disappeared in the metacyclic stages as TcNaa15 localized to the kinetoplast (Supplementary Fig. S3B). Tissue culture trypomastigotes exhibited a more diffuse cytoplasmic localization and expression was reduced to a structure resembling the remaining short flagellum in amastigotes (Supplementary Fig. S3B).

3.7 TcNaa30/TcNaa38 and TcNaa10/TcNaa15 co-sediment with the ribosome.

We examined the TcNaC co-sedimentation with the ribosome through a sucrose cushion, and as shown in (Figure 4(A)), TcNaa30 is present in both the ribosomal and non-ribosomal fractions. A smaller amount of TcNaa38 could also be observed in the polysome fraction. The results for TcNatA (Figure 4(B)) showed the presence of TcNaa10 and TcNaa15 in both the ribosomal and non-ribosomal fractions. Anti-TcNaa15 detected an additional band of approximately 54 kDa in the ribosomal fraction. In contrast, anti-TcNaa10 detected a band of about the same size in the non-polysome fraction. The identity of the extra band is not known. Taken together, the ribosomal co-sedimentation results indicated that the TcNatA and TcNatC proteins might associate with the ribosomes.

371 3.8 *T. cruzi* NatC and TcNatA subunits interact *in vivo* and *in vitro*.

372 Human orthologs of TcNaa30, TcNaa35 and TcNaa38 form a stable complex *in vivo*
373 (8). To investigate whether TcNaa30 and TcNaa38 formed a stable complex in *T.*
374 *cruzi*, immunoprecipitation using anti TcNaa30 and anti TcNaa38 was performed.
375 Immunoprecipitation with anti-TcNaa30 was unsuccessful, but using anti-TcNaa38
376 we were able to immunoprecipitate TcNaa30 (Figure 5(A)). Though further study is
377 required, this indicates that these proteins physically interact in *T. cruzi*, either
378 directly or through another protein, for example, the ribosome complex. Likewise,
379 immunoprecipitation showed that anti-TcNaa10 was able to immunoprecipitate
380 TcNaa15 (Figure 5(B)) upper panel. By reciprocal immunoprecipitation, anti-
381 TcNaa15 was able to pull down TcNaa10, (Figure 5(B)) lower panel. This analysis
382 suggests that the TcNaa10 and TcNaa15 interact *in vivo* in the same way as yeast and
383 human orthologs of the TcNaa10 and TcNaa15 form a stable complex *in vitro* and *in*
384 *vivo* (7)(9)(29).

385 3.9 *In vitro* Na-acetyltransferase assay.

386 In order to investigate the substrate specificity of TcNatC and TcNatA, we performed
387 an *in vitro* Nt-acetylation assay where purified recombinant protein (GST-TcNaa30)
388 was incubated with synthetic peptides representing substrates for different classes of
389 NATs (NatA-NatE). As shown in (Figure 6), TcNaa30 preferentially acetylates a
390 peptide with a hydrophobic N-terminal sequence of MLGP, which corresponds to a
391 typical NatC/E/F substrate in humans. We also attempted to assess TcNaa10
392 enzymatic activity, and whether the TcNaa10 substrate preferences are identical to
393 those in human cells in a similar way as above. Though there was an indication of
394 Naa10 activity, preferentially acetylating the synthetic peptide sequences STPD and
395 EEEIA (not shown), representing human NatA substrates, no reproducible activity
396 was found.

398 3.10 Effect of knock down of predicted *T. brucei* NatC catalytic subunit by RNAi.

399 RNAi was carried out on the *T. brucei* equivalent of the TcNaa30 gene. RNAi was
400 induced in *Trypanosoma brucei brucei* 427 using tetracycline. For the wild type,
401 tetracycline had no effect on their viability (Supplementary Fig. S5A).

~~For the transfectants, significantly reduced growth was observed in both the induced and non-induced after 48h and 72h.~~

We observed a ~~significant~~ a reduction in parasite growth **in both the induced and non-induced after 48 h and 72 h (not shown Supplementary Fig. S5B and S5C). This indicated that the RNAi vector was leaky.** An RT-PCR assay (~~not shown Supplementary Fig. S5D~~) indicated that at 48 h post induction, there was a decrease in the levels of endogenous mRNA in the induced and non-induced trans-formant cell compared to the wild type. Western blotting using anti- *T. cruzi* NatC (TcNaa30) showed that, especially after 48 h, there was lower protein expression in the non-induced and induced cells compared to the wild type (Fig. 7).

4. Discussion

We here describe the molecular cloning and characterization of the predicted *T. cruzi* NatC and *T. cruzi* NatA Na⁺-acetyltransferase protein complexes. We found that protein Nt-acetylation by *T. cruzi* NatC and NatA was similar to what has been described in other eukaryotes. It appears that the expression profile of TcNatA and TcNatC in different parasite life cycle is not uniform. But, how this translates to the distinct parasite morphologies and biology is not clear. Similar to expression, the localization profile of TcNatC and TcNatA proteins by immunofluorescence in the different life cycle forms are diverged. The functional significance of these, are speculated. Similar staining patterns were observed (16)(30)(31) for human Naa40/NatD and other NATs proteins. Given the divergent expression and localization of the TcNatC and TcNatA proteins, it is tempting to speculate that, the given protein is located at a particular compartment at a given time to carry biological tasks. Considering localization of *T. brucei* (Tb927.7.2360) a similar gene to TcNaa30 by GFP-tagged version (32), the *T. brucei* gene N-terminally and C-terminally tagged versions are distributed throughout the cell. Localization of TcNaa30 in our hands is predominantly distributed in the cytoplasm, suggesting differential biological function in trypanosomes. Further analyses are needed to confirm this hypothesis.

TcNatC and TcNatA proteins physically interact with each other and it is plausible that this interaction takes place in the cytoplasm as suggested by their possible ribosomal co-sedimentation. Possibly, the proteins in some cases carry out their

function independently of each other as suggested in other organisms (16), and that they may have specific functions depending on the parasite life cycle stage. TcNatC/TcNatA proteins may also have other functions independent of the NAT-activity as suggested in other species (15).

The biological significance of post-translational modification of proteins, especially acetylation, in trypanosomes is relatively unexplored (33). We predicted the TcNatC substrates profile and detected many parasite-specific proteins that lack homologues in humans (Table 2). For TcNatA substrates, the predictions include hypothetical proteins, as well as mucin-associated surface protein (MASP) and mucin proteins (not shown). The MASP gene family is preferentially expressed in the trypomastigote (34). Moreover, it is exposed to the host immune system and possibly used by the parasite during infection (34). Another noticeable predicted *T. cruzi* NatC and TcNatA substrate is trans-sialidase (TS); a polymorphic surface enzyme used by the parasite during infection (35). Taken together, it can be speculated that Nt-acetylation, if lost, could simultaneously affect many surface antigens including TS, or many parasite-specific functions and cellular processes that are important for pathology.

For the extracellular parasite *T. brucei*, some proteins used by the parasite to evade the host immune system were predicted as possible substrates for TbNatC (not shown). These include receptor-like adenylate cyclases (36), variant surface glycoprotein and an expression site- associated gene (37). Study of the N-terminal acetylome by proteomic methods in trypanosomes (33) confirms our prediction that, Nt-acetylation state in these organisms is common. Further studies are required for a complete understanding of which cellular machineries are regulated this way and how this is important for the life of the parasite.

In yeast, human and plants, the biological significance of NatC knockdown has been investigated (38)(8)(39). These studies point towards loss of cell viability if NatC is depleted. The NatA protein complex was found to be essential for cell survival in *T. brucei* (18). Given the sequence identity, and the similar predicted ligand binding and active sites, it is likely that NatA is essential in all trypanosomatids. In this study, silencing of the *T. brucei* NatC predicted catalytic subunit by RNAi suggests that the protein may be important to the parasite, though there was minor reduction of the predicted protein band in the blot in the transfected cells compared with the control.

Another system for conditional knockouts for trypanosomatids such as CRISPR/Cas9 could be tested to ascertain our observation in this study. Or, perform genome-scale RNAi (40) by silencing the parasites NATs catalytic subunits and phenotypes assessed. It is clear though, that, these are basic, important functions that are of interest for gene function and regulation as well as for possible drug target testing.

Collectively, identification of all the NATs in *T. cruzi*, analyzing substrates preferences and proteomic study of Nt-acetylation in all the developmental stages will narrow the gaps in knowledge of the parasite biology.

Acknowledgements

We thank Florian A. Salomons for helping us with confocal microscopy. We are also in debt to Daniela F. Gradia of Instituto de Biologia Molecular do Paraná, Brazil for providing us with anti- *T. cruzi* ribosomal protein S7 and Jacqueline Búa of Instituto Nacional de Parasitología, Buenos Aires, Argentina for providing us with anti- *T. cruzi* cyclophilin A. This study was supported by European Union grant “Chagas-Epinet” and the Swedish Research Council. The financier has got no control over study design, data analyses and manuscript preparation.

Competing interests: We declare that there are no competing interests.

Authors' contributions: SO, BA and LA conceived the studies. SO put forward the study plan, co-ordinated the studies, performed experiments and bioinformatics, and drafted the manuscript. OF led the bioinformatics analyses and contributed in drafting the manuscript. DB and EM coordinated and participated in the RNAi study. HF, SS and TA, performed in vitro acetylation assays. CB and KT prepared parasite extracts and undertook immunofluorescence analyses. All authors participated in analysis of the results and refinement of the draft.

References

1. Rassi, A., Rassi, A., and Marin-Neto, J. A. (2010) Chagas disease. *Lancet*. **375**, 1388–1402
2. Brun, R., Blum, J., Chappuis, F., and Burri, C. (2010) Human African

496 trypanosomiasis. *Lancet*. **375**, 148–159

497 3. Wilkinson, S. R., Taylor, M. C., Horn, D., Kelly, J. M., and Cheeseman, I.
 498 (2008) A mechanism for cross-resistance to nifurtimox and benznidazole in
 499 trypanosomes. *Proc. Natl. Acad. Sci.* **105**, 5022–5027

500 4. Barrett, M. P., Vincent, I. M., Burchmore, R. J., Kazibwe, A. J., and Matovu,
 501 E. (2011) Drug resistance in human African trypanosomiasis. *Future*
 502 *Microbiol.* **6**, 1037–1047

503 5. Falb, M., Aivaliotis, M., Garcia-Rizo, C., Bisle, B., Tebbe, A., Klein, C.,
 504 Konstantinidis, K., Siedler, F., Pfeiffer, F., and Oesterhelt, D. (2006) Archaeal
 505 N-terminal Protein Maturation Commonly Involves N-terminal Acetylation: A
 506 Large-scale Proteomics Survey. *J. Mol. Biol.* **362**, 915–924

507 6. Drazic, A., Aksnes, H., Marie, M., Boczkowska, M., Varland, S., Timmerman,
 508 E., Foy, H., Glomnes, N., Rebowski, G., Impens, F., Gevaert, K., Dominguez,
 509 R., and Arnesen, T. (2018) NAA80 is actin's N-terminal acetyltransferase and
 510 regulates cytoskeleton assembly and cell motility. *Proc. Natl. Acad. Sci.*
 511 10.1073/pnas.1718336115

512 7. Arnesen, T., Anderson, D., Baldersheim, C., Lanotte, M., Varhaug, J. E., and
 513 Lillehaug, J. R. (2005) Identification and characterization of the human ARD1-
 514 NATH protein acetyltransferase complex. *Biochem. J.* **386**, 433–443

515 8. Starheim, K. K., Gromyko, D., Evjenth, R., Ryningen, A., Varhaug, J. E.,
 516 Lillehaug, J. R., and Arnesen, T. (2009) Knockdown of human N alpha-
 517 terminal acetyltransferase complex C leads to p53-dependent apoptosis and
 518 aberrant human Arl8b localization. *Mol. Cell. Biol.* **29**, 3569–81

519 9. Gautschi, M., Just, S., Mun, A., Ross, S., Rucknagel, P., Dubaquitte, Y.,
 520 Ehrenhofer-Murray, A., and Rospert, S. (2003) The Yeast N -Acetyltransferase
 521 NatA Is Quantitatively Anchored to the Ribosome and Interacts with Nascent
 522 Polypeptides. *Mol. Cell. Biol.* **23**, 7403–7414

523 10. Arnesen, T. (2011) Towards a functional understanding of protein N-terminal
 524 acetylation. *PLoS Biol.* 10.1371/journal.pbio.1001074

525 11. Kalvik, T. V., and Arnesen, T. (2013) Protein N-terminal acetyltransferases in
 526 cancer. *Oncogene*. **32**, 269–276

527 12. Hwang, C. S., Shemorry, A., and Varshavsky, A. (2010) N-terminal acetylation
 528 of cellular proteins creates specific degradation signals. *Science (80-.)*. **327**,
 529 973–977

530 13. Scott, D. C., Monda, J. K., Bennett, E. J., Harper, J. W., and Schulman, B. A.
 531 (2011) N-terminal acetylation acts as an avidity enhancer within an
 532 interconnected multiprotein complex. *Science (80-.)*. **334**, 674–678

533 14. Forte, G. M. A., Pool, M. R., and Stirling, C. J. (2011) N-terminal acetylation
 534 inhibits protein targeting to the endoplasmic reticulum. *PLoS Biol.*
 535 10.1371/journal.pbio.1001073

- 536 15. Arnesen, T., Thompson, P. R., Varhaug, J. E., and Lillehaug, J. R. (2008) The
537 protein acetyltransferase ARD1: a novel cancer drug target? *Curr. Cancer Trug*
538 *targets*. **8**, 545–553
- 539 16. van Damme, P., Hole, K., Pimenta-Marques, A., Helsens, K., Vandekerckhove,
540 J., Martinho, R. G., Gevaert, K., and Arnesen, T. (2011) NatF contributes to an
541 evolutionary shift in protein N-terminal acetylation and is important for normal
542 chromosome segregation. *PLoS Genet.* 10.1371/journal.pgen.1002169
- 543 17. Arnesen, T., Van Damme, P., Polevoda, B., Helsens, K., Evjenth, R., Colaert,
544 N., Varhaug, J. E., Vandekerckhove, J., Lillehaug, J. R., Sherman, F., and
545 Gevaert, K. (2009) Proteomics analyses reveal the evolutionary conservation
546 and divergence of N-terminal acetyltransferases from yeast and humans. *Proc.*
547 *Natl. Acad. Sci.* **106**, 8157–8162
- 548 18. Ingram, a K., Cross, G. a, and Horn, D. (2000) Genetic manipulation indicates
549 that ARD1 is an essential N(infinity)-acetyltransferase in *Trypanosoma brucei*.
550 *Mol. Biochem. Parasitol.* **111**, 309–317
- 551 19. Ochaya, S., Respuela, P., Simonsson, M., Saraswathi, A., Branche, C., Lee, J.,
552 Búa, J., Nilsson, D., Åslund, L., Bontempi, E. J., and Andersson, B. (2007)
553 Characterization of a *Trypanosoma cruzi* acetyltransferase: cellular location,
554 activity and structure. *Mol. Biochem. Parasitol.* **152**, 123–131
- 555 20. Isola, E. L. D., Lammel, E. M., and Cappa, S. M. G. (1986) *Trypanosoma*
556 *cruzi*: Differentiation after interaction of epimastigotes and *Triatoma infestans*
557 intestinal homogenate. *Exp. Parasitol.* **62**, 329–335
- 558 21. Tyler, K. M., and Engman, D. M. (2000) Flagellar elongation induced by
559 glucose limitation is preadaptive for *Trypanosoma cruzi* differentiation. *Cell*
560 *Motil. Cytoskeleton.* **46**, 269–278
- 561 22. Polevoda, B., Arnesen, T., and Sherman, F. (2009) A synopsis of eukaryotic
562 N α -terminal acetyltransferases: nomenclature, subunits and substrates. *BMC*
563 *Proc.* **3**, S2
- 564 23. Seo, J. H., Cha, J. H., Park, J. H., Jeong, C. H., Park, Z. Y., Lee, H. S., Oh, S.
565 H., Kang, J. H., Suh, S. W., Kim, K. H., Ha, J. Y., Han, S. H., Kim, S. H., Lee,
566 J. W., Park, J. A., Jeong, J. W., Lee, K. J., Oh, G. T., Lee, M. N., Kwon, S. W.,
567 Lee, S. K., Chun, K. H., Lee, S. J., and Kim, K. W. (2010) Arrest defective 1
568 autoacetylation is a critical step in its ability to stimulate cancer cell
569 proliferation. *Cancer Res.* **70**, 4422–4432
- 570 24. D’Andrea, L. D., and Regan, L. (2003) TPR proteins: The versatile helix.
571 *Trends Biochem. Sci.* **28**, 655–662
- 572 25. Frangioni, J. V., and Neel, B. G. (1993) Solubilization and purification of
573 enzymatically active glutathione S-transferase (pGEX) fusion proteins. *Anal.*
574 *Biochem.* **210**, 179–187
- 575 26. Myburgh, E., Coles, J. A., Ritchie, R., Kennedy, P. G. E., McLatchie, A. P.,
576 Rodgers, J., Taylor, M. C., Barrett, M. P., Brewer, J. M., and Mottram, J. C.

- 577 (2013) In vivo imaging of trypanosome-brain interactions and development of
578 a rapid screening test for drugs against CNS stage trypanosomiasis. *PLoS Negl.*
579 *Trop. Dis.* 10.1371/journal.pntd.0002384
- 580 27. Radwanska, M., Chamekh, M., Vanhamme, L., Claes, F., Magez, S., Magnus,
581 E., De Baetselier, P., Büscher, P., and Pays, E. (2002) The serum resistance-
582 associated gene as a diagnostic tool for the detection of *Trypanosoma brucei*
583 *rhodesiense*. *Am. J. Trop. Med. Hyg.* 10.4269/ajtmh.2002.67.684
- 584 28. Teixeira, D. E., Benchimol, M., Crepaldi, P. H., and de Souza, W. (2012)
585 Interactive Multimedia to Teach the Life Cycle of *Trypanosoma cruzi*, the
586 Causative Agent of Chagas Disease. *PLoS Negl. Trop. Dis.*
587 10.1371/journal.pntd.0001749
- 588 29. Park, E. C., and Szostak, J. W. (1992) ARD1 and NAT1 proteins form a
589 complex that has N-terminal acetyltransferase activity. *EMBO J.* **11**, 2087–93
- 590 30. Hole, K., van Damme, P., Dalva, M., Aksnes, H., Glomnes, N., Varhaug, J. E.,
591 Lillehaug, J. R., Gevaert, K., and Arnesen, T. (2011) The human N-Alpha-
592 acetyltransferase 40 (hNaa40p/hNatD) is conserved from yeast and N-
593 terminally acetylates histones H2A and H4. *PLoS One*.
594 10.1371/journal.pone.0024713
- 595 31. Ren, T., Jiang, B., Jin, G., Li, J., Dong, B., Zhang, J., Meng, L., Wu, J., and
596 Shou, C. (2008) Generation of novel monoclonal antibodies and their
597 application for detecting ARD1 expression in colorectal cancer. *Cancer Lett.*
598 **264**, 83–92
- 599 32. Dean, S., Sunter, J. D., and Wheeler, R. J. (2017) TrypTag.org: A
600 Trypanosome Genome-wide Protein Localisation Resource. *Trends Parasitol.*
601 10.1016/j.pt.2016.10.009
- 602 33. Moretti, N. S., Cestari, I., Anupama, A., Stuart, K., and Schenkman, S. (2017)
603 Comparative proteomic analysis of lysine acetylation in Trypanosomes. *J.*
604 *Proteome Res.* 10.1021/acs.jproteome.7b00603
- 605 34. Bartholomeu, D. C., Cerqueira, G. C., Leão, A. C. A., daRocha, W. D., Pais, F.
606 S., Macedo, C., Djikeng, A., Teixeira, S. M. R., and El-Sayed, N. M. (2009)
607 Genomic organization and expression profile of the mucin-associated surface
608 protein (masp) family of the human pathogen *Trypanosoma cruzi*. *Nucleic*
609 *Acids Res.* **37**, 3407–3417
- 610 35. Freitas, L. M., dos Santos, S. L., Rodrigues-Luiz, G. F., Mendes, T. A. O.,
611 Rodrigues, T. S., Gazzinelli, R. T., Teixeira, S. M. R., Fujiwara, R. T., and
612 Bartholomeu, D. C. (2011) Genomic analyses, gene expression and antigenic
613 profile of the trans-sialidase superfamily of *trypanosoma cruzi* reveal an
614 undetected level of complexity. *PLoS One*. 10.1371/journal.pone.0025914
- 615 36. Salmon, D., Vanwalleghem, G., Morias, Y., Denoeud, J., Krumbholz, C.,
616 Lhomme, F., Bachmaier, S., Kador, M., Gossmann, J., Dias, F. B. S., De
617 Muylder, G., Uzureau, P., Magez, S., Moser, M., De Baetselier, P., Van Den

618 Abbeelee, J., Beschin, A., Boshart, M., and Pays, E. (2012) Adenylate cyclases
619 of *Trypanosoma brucei* inhibit the innate immune response of the host. *Science*
620 (80-.). **337**, 463–466

621 37. Berriman, M., Ghedin, E., Hertz-Fowler, C., Blandin, G., Renauld, H.,
622 Bartholomeu, D. C., Lennard, N. J., Caler, E., Hamlin, N. E., Haas, B., Böhme,
623 U., Hannick, L., Aslett, M. A., Shallom, J., Marcello, L., Hou, L., Wickstead,
624 B., Alsmark, U. C. M., Arrowsmith, C., Atkin, R. J., Barron, A. J., Bringaud,
625 F., Brooks, K., Carrington, M., Cherevach, I., Chillingworth, T. J., Churcher,
626 C., Clark, L. N., Corton, C. H., Cronin, A., Davies, R. M., Doggett, J., Djikeng,
627 A., Feldblyum, T., Field, M. C., Fraser, A., Goodhead, I., Hance, Z., Harper,
628 D., Harris, B. R., Hauser, H., Hostetler, J., Ivens, A., Jagels, K., Johnson, D.,
629 Johnson, J., Jones, K., Kerhornou, A. X., Koo, H., Larke, N., Landfear, S.,
630 Larkin, C., Leech, V., Line, A., Lord, A., MacLeod, A., Mooney, P. J., Moule,
631 S., Martin, D. M. A., Morgan, G. W., Mungall, K., Norbertczak, H., Ormond,
632 D., Pai, G., Peacock, C. S., Peterson, J., Quail, M. A., Rabinowitsch, E.,
633 Rajandream, M. A., Reitter, C., Salzberg, S. L., Sanders, M., Schobel, S.,
634 Sharp, S., Simmonds, M., Simpson, A. J., Tallon, L., Turner, C. M. R., Tait,
635 A., Tivey, A. R., Van Aken, S., Walker, D., Wanless, D., Wang, S., White, B.,
636 White, O., Whitehead, S., Woodward, J., Wortman, J., Adams, M. D., Embley,
637 T. M., Gull, K., Ullu, E., Barry, J. D., Fairlamb, A. H., Opperdoes, F., Barrell,
638 B. G., Donelson, J. E., Hall, N., Fraser, C. M., Melville, S. E., and El-Sayed, N.
639 M. (2005) The genome of the African trypanosome *Trypanosoma brucei*.
640 *Science* (80-.). **309**, 416–422

641 38. Polevoda, B., and Sherman, F. (2001) NatC N α -terminal Acetyltransferase of
642 Yeast Contains Three Subunits, Mak3p, Mak10p, and Mak31p. *J. Biol. Chem.*
643 **276**, 20154–20159

644 39. Pesaresi, P., Gardner, N. a, Masiero, S., Dietzmann, A., Eichacker, L.,
645 Wickner, R., Salamini, F., and Leister, D. (2003) Cytoplasmic N-terminal
646 protein acetylation is required for efficient photosynthesis in Arabidopsis.
647 *Plant Cell*. **15**, 1817–1832

648 40. Glover, L., Alsford, S., Baker, N., Turner, D. J., Sanchez-Flores, A.,
649 Hutchinson, S., Hertz-Fowler, C., Berriman, M., and Horn, D. (2015) Genome-
650 scale RNAi screens for high-throughput phenotyping in bloodstream-form
651 African trypanosomes. *Nat. Protoc.* 10.1038/nprot.2015.005

652

653

654

655

656

657

658
659
660
661
662
663
664
665
666
667
668
669
670
671
672
673
674

675 **Table 1.** TcNatC and TcNatA genes. * Denote genes investigated in this study.

TcNat	Gene	CL Brener haplotype
TcNatC catalytic subunit (TcNaa30)	Tc00.1047053511809.120 (Tc9.120)	Non- Esmeraldo-like *
	Tc00.1047053511811.30 (Tc1.30)	Esmeraldo- like
TcNatC auxiliary subunit (TcNaa35)	Tc00.1047053511311.80 (Tc1.80)	Esmeraldo- like
	Tc00.1047053511755.119 (Tc5.119)	Non- Esmeraldo-like *
TcNatC auxiliary subunit (TcNaa38)	Tc00.1047053507209.10 (Tc9.10)	Non- Esmeraldo-like *
TCNatA catalytic subunit (TcNaa10)	TcCLB.506227.230 (Tc7.230)	Esmeraldo-like *
TCNatA auxiliary subunit (TcNaa15)	TcCLB.504163.110 (Tc3.110)	Esmeraldo-like
	TcCLB.510301.80 (Tc01.80)	Non-Esmeraldo-like *

676

677 **Table 2.** Some estimated number of predicted TcNaa30 substrates for CL Brener
678 haplotypes based on Met-Leu, Met-Ile, Met-Phe and Met-Tyr N-termini.

	Non-Esmeraldo	Esmeraldo
Total genes	1461	1328
hypothetical	830	774
trans-sialidase	248	203
mucin TcMUCII	2	2
MASP	4	3

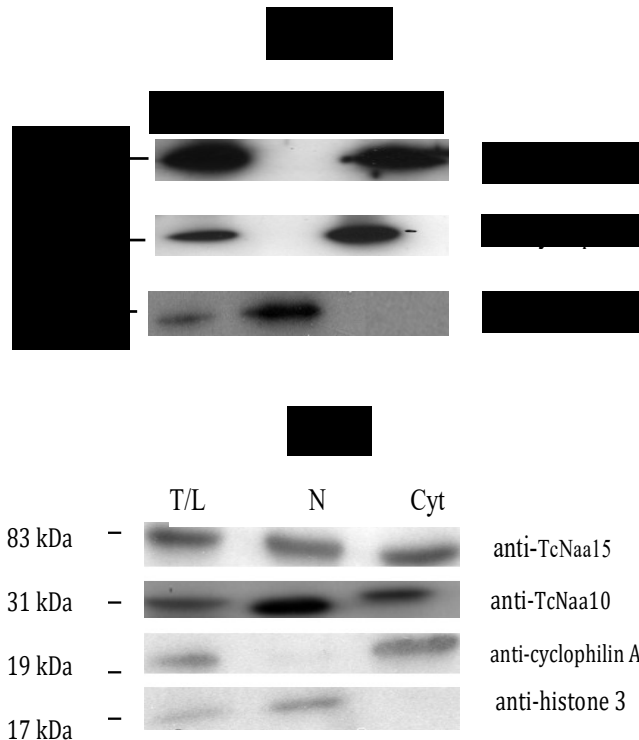
679
680
681
682
683
684
685
686
687
688
689
690
691
692
693
694
695
696
697
698
699
700



Figure 1: Expression of TcNaa38/TcNaa30 and TcNaa10/TcNaa15 in trypanosomes.

A; Total proteins from different stages of *T. cruzi* life cycle, epimastigote midlog (M), epimastigote stationary phase (S), trypomastigote (T) and amastigote (A) were used for western blotting. **B;** Cross reaction of anti-TcNaa30 and anti-TcNaa38 against different *T. brucei* strains. Tb-Gvr (*T. brucei* GVR strain), Tb-R17 (*T. brucei* R17 strain) and Tc-Brener epimastigote (*T. cruzi* CL Brener strain). **C;** Developmental stage expression of TcNaa10 and TcNaa15 in CL Brener strain epimastigote (E), trypomastigote (T) and amastigote (A). Purified anti-TcNaa10 and anti-TcNaa15 (1:4000, and 1: 2000 dilutions) were used for western blotting. **D;** Cross reaction of anti-TcNaa10 (upper panel) and anti- TcNaa15 (lower panel) against different *T. brucei* strains. Strains used are as in **B**.

716
717
718
719



720
721

722 **Figure 2:** Localisation of TcNaa30 and TcNaa10/TcNaa15 in *T. cruzi*. **A;** TcNaa30
723 localization in epimastigotes by western blotting. **B;** Localization of
724 TcNaa10/TcNaa15. Cytoplasmic (Cyt) and nuclear (N) fractions were assessed for the
725 presence of TcNaa30, TcNaa10 and TcNaa15. Anti- cyclophilin A and anti-histone 3,
726 were used as positive controls for cytoplasmic and nuclear protein, respectively. T/L
727 indicates total cell lysate.

728

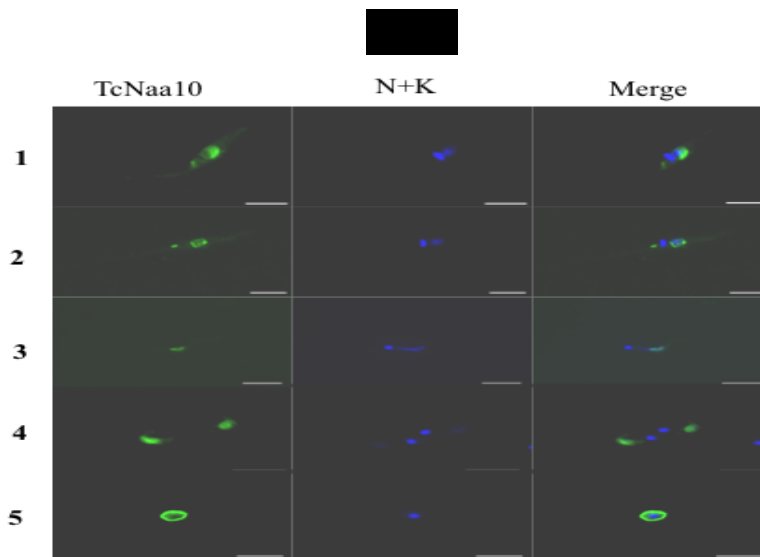
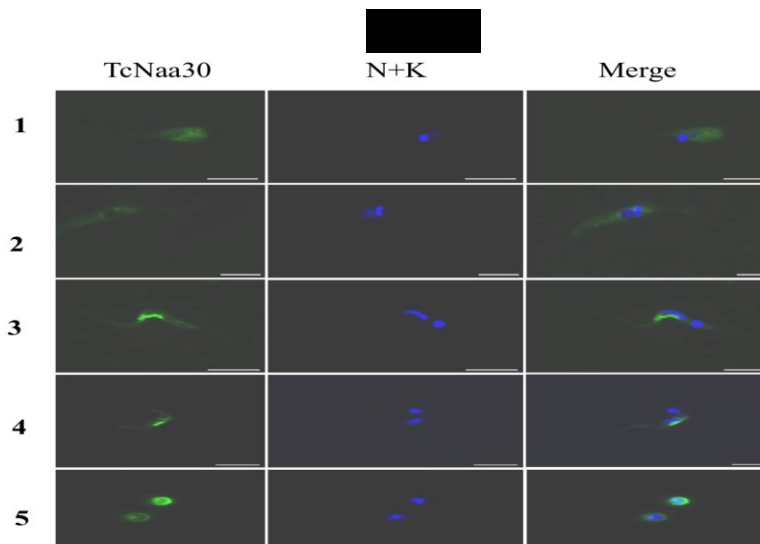


Figure 3: Localization of TcNaa30 and TcNaa10 by immunolabelling. Number 1 to 5 denotes, Midlog epimastigotes, Stationary epimastigotes, Metacyclic trypomastigotes, Trypomastigotes, and Amastigotes, respectively. *T. cruzi* four life cycle stages were immunolabelled with, **A**; anti-TcNaa30 and **B**; anti-TcNaa10. The nucleus and kinetoplast were visualized using DAPI stain (N+K), scale bars = 5µm.

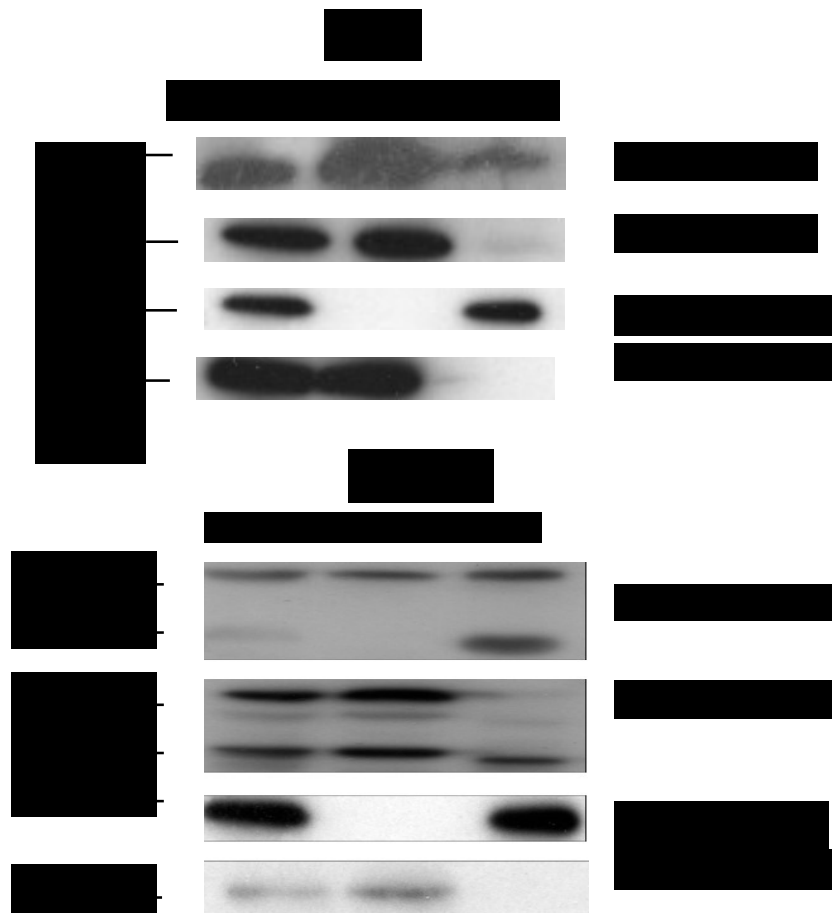
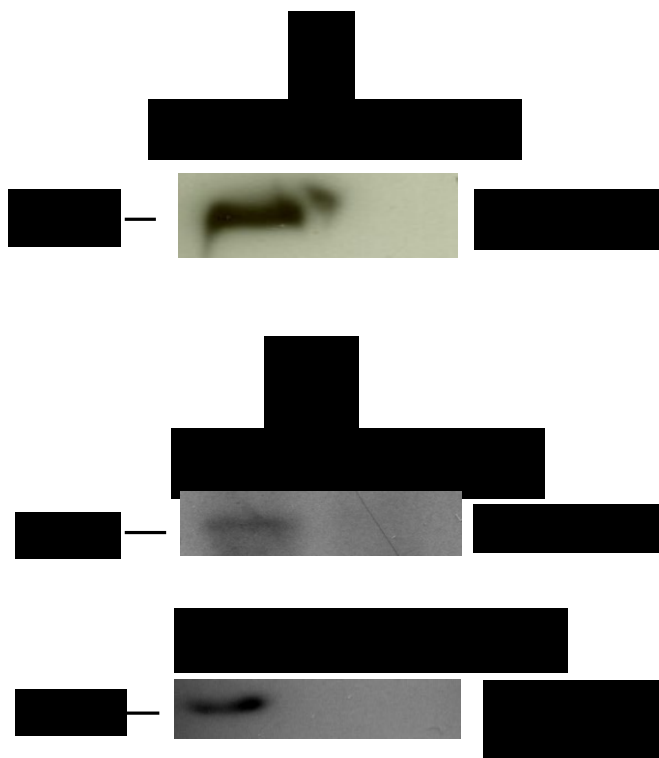


Figure 4: Association of TcNaa30 /TcNaa38 and TcNaa10/TcNaa15 with the ribosome. **A;** Membrane was incubated with anti TcNaa30 and anti TcNaa38. Total cell lysate (T/L), supernatant post-ultracentrifugation (P/L) and polysomes (Poly) were loaded. As controls, anti-*T. cruzi* S7 (specific for the ribosome) and anti- *T. cruzi* cyclophilin A (non-ribosomal) were used. Molecular size markers in kDa are indicated on the left. **B;** Membrane was incubated with anti TcNaa10 and TcNaa15. Loading control as mentioned in Fig. 4A.



745

746 **Figure 5:** TcNatC and TcNatA protein interaction. **A;** Immunoprecipitation (IP) of
 747 TcNaa30. The parasite lysate was incubated with anti-TcNaa38. As a control, the
 748 lysate was incubated with rabbit sera (pre-immune). The blot was analyzed with anti-
 749 TcNaa30. Molecular weight marker in kDa is indicated. **B;** Co- Immunoprecipitation
 750 assays of TcNaa10 with TcNaa15 protein. IP with pre- immune sera was used as a
 751 control. Western blots of the immunoprecipitated samples were probed with rabbit
 752 anti-TcNaa10 and anti-TcNaa15.

753
 754
 755
 756
 757
 758
 759
 760
 761
 762

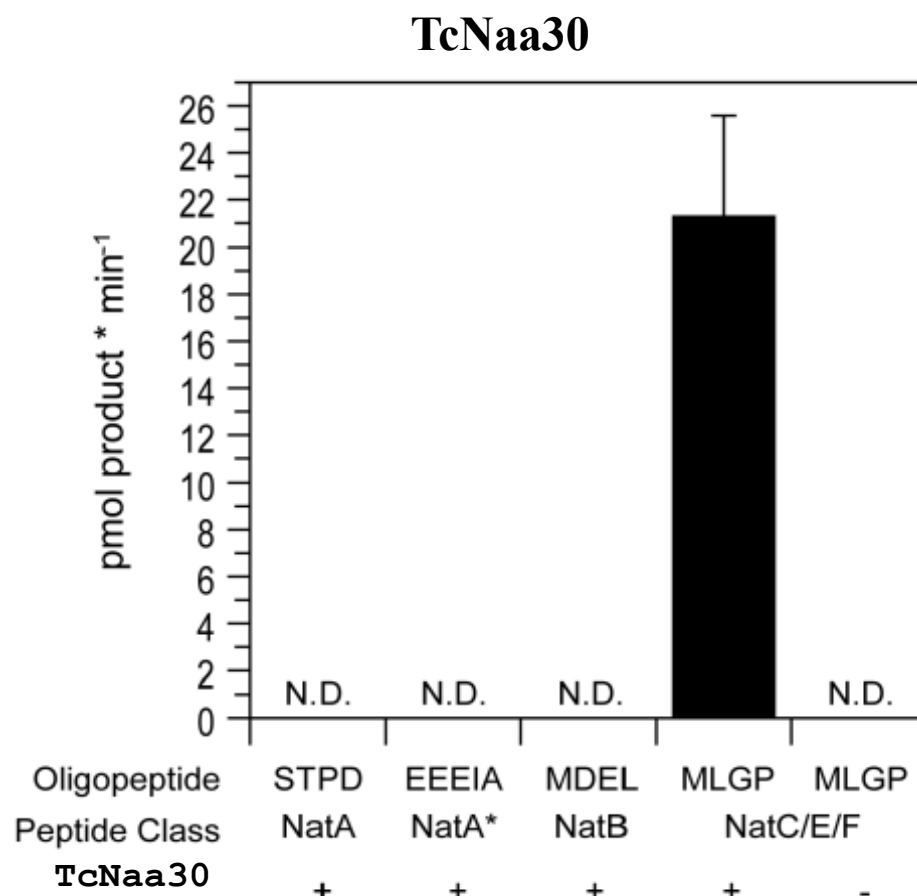


Figure 6: *In vitro* acetyltransferase activity of TcNaa30. GST-TcNaa30 was incubated with acetyl-CoA (300 mM) and selected oligopeptides (300 mM) for 30 min at 37 °C. dH₂O was used as negative control. The amount of acetylated peptide was determined with reverse phase HPLC. Oligopeptide names indicate the first four amino acids from the N-terminus. N.D represent non- detectable. The * indicates that NatA can also post-translationally acetylate acidic N termini, for example γ actin.

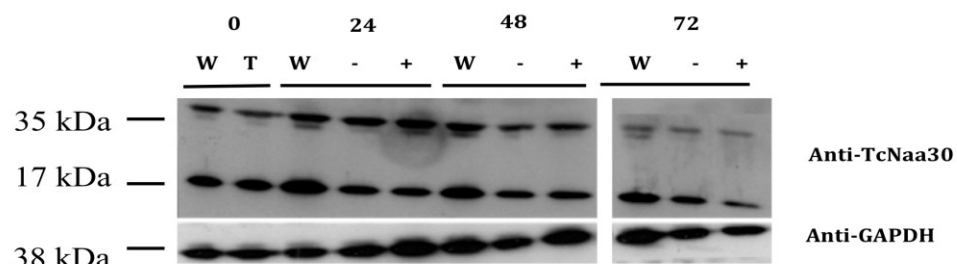


Figure 7: Phenotype of the knock down of putative *T. brucei* Naa30 by RNAi. TcNaa30 protein expression analysis of wild type (W), transformant (T), non-induced (-) and induced (+) cells by western blotting. Cells were counted, washed, dissolved in sample buffer and immediately boiled. About equal amount of each sample was used in the experiment. Note that a band of about 17 kDa, whose identity is not known, was also identified. GAPDH was used as loading control.